Joint multi-target detection and localization with a noncoherent statistical MIMO radar

Yue Ai*, Wei Yi*, Mark R. Morelande† and Lingjiang Kong*
*School of Electronic Engineering, University of Electronic Science and Technology of China
E-mail: {kussoyi, lingjiang.kong}@gmail.com
†Melbourne Systems Lab, University of Melbourne, Australia
E-mail: mrmore@unimelb.edu.au

***Abstract*—In this paper, the problems of simultaneously detecting and localizing multiple targets are considered for noncoherent multiple-input multiple-output (MIMO) radar with widely separated antennas. By assuming a prior knowledge of target number, an optimal solution to this problem is presented first. It is essentially a maximum-likelihood (ML) estimator searching parameters of interest in a high-dimensional space. However, the complexity of this method increases exponentially with the number of targets. Besides, without the prior information of target number, a multi-hypothesis test strategy on target number is required, which further complicates this method. Therefore, we split the joint maximization into *G* disjoint optimization problems by clearing the interference from previously declared targets. In this way, we derive two fast but robust suboptimum solutions which allow trading performance for a much lower implementation complexity which is almost independent of the number of targets. In addition, the multi-hypothesis test detector is no longer required when target number is unknown. Simulation results show the proposed suboptimum algorithms can correctly detecting and accurately localizing multiple targets even when targets share common range bin in some paths.**

Keywords—noncoherent statistic MIMO radar; maximum-likelihood estimation (MLE); multitarget detection and localization; high-dimensional estimation

I. INTRODUCTION

Recently, multiple-input multiple-output (MIMO) radar, whose concept is brought from wireless communication field, has drawn more and more attention from researchers. Due to the different mode of placement of antennas, generally MIMO radar can be classified into two categories. The first category co-located MIMO radar with closely spaced antennas is similar to conventional phase array radar [1]. The second category, known as statistical MIMO radar, employs widely separated antennas. It has been shown that contributing to both transmitted waveforms and spatial diversity, statistical MIMO radar can mitigate the performance degradations caused by the radar cross-section fluctuations [2]-[3], and thus proving both diversity gain and geometry gain leading to the improvement of localization performance [4].

As for statistical MIMO radar, basically there are two kinds of target localization methods, one is based on the measurements of the estimated propagated delay or the angle of arrival at the receiver [5], and the other one is based on received radar signal before detection process for maximum-likelihood estimation (MLE) [6]-[9]. The methods belonging to the latter group make the most use of target information, and thus lead to a potentially higher accuracy especially for weak targets. Its basic idea is to obtain the estimated location of target by searching for the coordinate position that maximize the likelihood ratio based on raw received signal, in the data plane. These methods are valid under the assumption that there is one and only one target in the data plane. As for multi-target scenario, simply expanding the searching dimension which increases exponentially in the number of targets is computationally prohibited, otherwise the global maximum degrades to local maximum, which calls for a detection process to decide the existence of these targets. Thus, a joint detection and localization algorithm is needed for multi-target.

Gorgri [10] has proposed a multiple-hypothesis (MH)-based algorithm for multi-target localization. In [11], we attempt to propose a fast multi-target localization algorithm without multiple hypothesis testing. With the utilization of connected region, the targets are localized in parallel in the original dimension of single target and thus reducing complexity. However, the assumption that targets are isolated in all the path is not always hold in realistic application and the multi-target localization performance relies on the setting of threshold which is not simply only a detection threshold but also a key point to separate the searching range of each target. Thus, the difficulty to obtain an appropriate threshold restricts its practical application. This method also requires a strong assumption that targets are always completely resolved.

In this paper, we deal with the problem of multi-target joint detection and localization for statistical MIMO radar. To this end, we start with an optimal high dimension localization method based on joint MLE and then derive a suboptimal algorithm by splitting the joint maximization into several disjoint optimization problems after eliminating the interference in all the paths from previously declared targets. This allows information of each target to be extracted one-by-one from the original received signal mingled with information of all targets, and then performing single target detection at each estimated location. Unlike our previous algorithm in [11], the threshold can be obtained based on theory of target detection and the algorithms declare targets serially. In addition, they remain efficient without the utilization of multi-hypothesis testing utilized in [10] when the prior knowledge of the number of targets is not available. In the scenario with completely resolved targets, the proposed algorithm is simplified further. Finally, numerical examples are provided to assess detection and localization performances of the proposed two multi-target localization algorithms.

II. Models and Notations

We assume a typical MIMO radar scenario with N transmitters located at $(x_k^t, y_k^t), (k=1,2,...,N)$, and M receivers located at (x_l^r, y_l^r), $(l=1,2,...,M)$ respectively, in a two-dimensional Cartesian coordinate system. The antennas of both transmitters and receivers are widely separated to ensure the space diversity. A set of mutually orthogonal signals are transmitted, with the lowpass equivalent $\sqrt{E/N}s_k(t)$, $k=1,2,...,N$ where E denotes the total transmitted energy for transmit antennas.

The focus in this paper is on simultaneously detecting and localizing targets, therefore only static targets are considered. Suppose that G ($G>1$) static targets appear in the radar surveillance region, with the g th target located at (x_g, y_g) .For convenience, we define a two-dimensioned vector $\boldsymbol{\theta}_g$ of the unknown location of the gth target

$$\boldsymbol{\theta}_g \triangleq [x_g, y_g]^T \tag{1}$$

For noncoherent MIMO radar, the received signal reflected from the gth target at lth receiver due to the signal transmitted from kth transmitter (defined as the lkth path) is given by (Considering the orthogonality of transmitted signals, an assumption is introduced that raw signal has been separated to N channels first, and each channel refers to the signal transmitted from a certain antenna):

$$r_{lkg}(t) = \sqrt{\frac{E}{N}}\alpha_{lkg} s_{kg}(t-\tau_{lkg}) + n_{lkg}(t), 0<t<T \tag{2}$$

where the reflection coefficient $\alpha_{lkg} = |\alpha_{lkg}|\exp(j\beta_{lkg})$ of the lkth path is a complex random variable. T is the observation time interval. $n_{lkg}(t)$ represents additive complex white Gaussian random noise. The propagation time between the kth transmitter and the lth receiver is

$$\tau_{lkg} = \frac{\sqrt{(x_g - x_k^t)^2 + (y_g - y_k^t)^2} + \sqrt{(x_g - x_l^r)^2 + (y_g - y_l^r)^2}}{c} \tag{3}$$

with c the speed of light.

Note that, to accommodate the more general case of moving targets, the signal model with target velocity taken into account can be found in [6].

After sampling, the continuous signal of (1) can be written in a vector form

$$\mathbf{r}_{lkg} = \sqrt{\frac{E}{N}}\alpha_{lkg}\tilde{\mathbf{s}}_{lkg} + \mathbf{n}_{lkg} \tag{4}$$

where

$$\mathbf{r}_{lkg} \triangleq [r_{lkg}[0], r_{lkg}[1], ..., r_{lkg}[N_T - 1]]^T \tag{5}$$

$$\tilde{\mathbf{s}}_{lkg} \triangleq [\tilde{s}_{lkg}[0], \tilde{s}_{lkg}[1], ..., \tilde{s}_{lkg}[N_T - 1]]^T \tag{6}$$

with a sampling interval $T_s = T/(N_T - 1)$, thus the sampled signal is $r_{lkg}[n] = r_{lk} g(nT_s)$, $\tilde{s}_{lkg}[n] = s_k(nT_s - \tau_{lkg})$. Note that $\tilde{\mathbf{s}}_{lkg}$ is the function of unknown location of target. The noise vectors $\mathbf{n}_{lkg}$ are normally distributed with zero mean and scaled identity covariance matrix $\sigma_{lkg}^2\mathbf{I}$.

Having taken all the reflections of the G targets into consideration, the vector form of the received signal of the lkth path in noncoherent processing is given below

$$\mathbf{r}_{lk} = \sum_{g=1}^{G}\sqrt{\frac{E}{N}}\alpha_{lkg}\tilde{\mathbf{s}}_{lkg} + \mathbf{n}_{lk} \tag{7}$$

where $\mathbf{n}_{lk}$ are mutually independent across different path and normally distributed with zero mean and a covariance matrix $\mathbf{R}_{lk}=\sigma_{lk}^2\mathbf{I}$.

III. Multi-target Detection and Localization

As discussed in [12], the MLE of the unknown parameter vector can be found by examining the likelihood ratio for the hypothesis pair, with H_1 corresponding to the target presence hypothesis and H_0 corresponding to the noise only hypothesis. As for multi-target estimation, the observation vector $\mathbf{r}_{lk}$ is related to the parameters of all targets ($\boldsymbol{\theta}_g, g=1,2,...,G$), thus a high dimensional parameter vector $\boldsymbol{\theta} = [\boldsymbol{\theta}_1^T, \boldsymbol{\theta}_2^T, ..., \boldsymbol{\theta}_G^T]^T \in S^G$ is introduced for the joint estimation of all targets.

Before proceeding, it is necessary to introduce the following Definition which is instrumental to the development of the subsequent algorithms.

Definition 1: Consider a scenario with G targets and a $M \times N$ MIMO radar, the gth ($g=1,2,...,G$) target is said to be *completely resolved*, if the time difference of arriving between this target and any other jth ($j=1,2,...,G$, $g \neq j$) target in any of the $M\times N$ paths is larger than the radar effective pulse width. That means,

$$|\tau_{lkg} - \tau_{lkj}| > \tau_c \tag{8}$$

where τ_{lkg} is the propagation time of gth target between the kth transmitter and l the receiver, and τ_c is the effective duration of the time-correlation of the transmitted waveform $s_k(t),\ k=1,2,...,N$ [12] (for example, if a rectangular pulse train is employed, then $\tau_c \simeq T_p$). Besides, the two targets g and j which satisfy (8) for the lkth path are referred as two *isolated targets* in the lkth path. Conversely, the gth target is called *unresolved* if (8) is not satisfied, indicating that the gth target shares with the jth target one range bin in the lkth path. By parity of reasoning, that any two of the G targets are mutually *isolated* in each of the $M\times N$ paths is defined as all the G targets are *completely resolved*, otherwise is defined as the G targets are *partially resolved*.

Take an $M\times N=2\times 2$ MIMO radar as an example, of which each antenna is monostatic, and also receiving signals transmitted from other antennas. A scenario with two unresolved targets is plotted in Fig.1 in which only two of the total four paths are plotted. It shows that the two targets are isolated in the AA path but unresolved in the BB path.

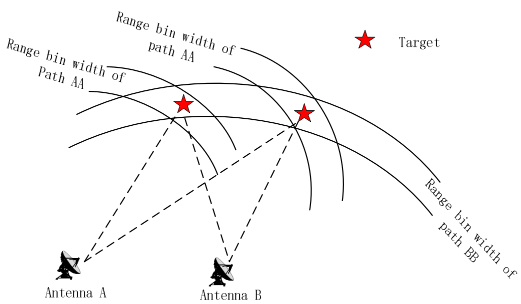

Fig. 1. Sketch map of a scenario with 2 targets and a 2×2 MIMO radar, wherein 2 targets are unresolved in the BBth path.

A. Optimal high-dimensional method

In order to simplify the problem, we assume that the target number G is known before localization. Assuming that H_1 represents the signal presence hypothesis as modeled in (7) and H_0 represents the noise-only hypothesis, the likelihood functions of $\mathbf{r}_{lk}$ under additive Gaussian white noise environment is

$$p(\mathbf{r}_{lk}|\boldsymbol{\theta},\ \boldsymbol{\alpha}_{lk},H_1)=C_1\exp\left\{-\frac{1}{2}\left(\mathbf{r}_{l,k}-\sum_{g=1}^{G}\sqrt{\frac{E}{N}}\alpha_{lkg}\tilde{\mathbf{s}}_{lkg}\right)^H \mathbf{R}_{lk}^{-1}\left(\mathbf{r}_{l,k}-\sum_{g=1}^{G}\sqrt{\frac{E}{N}}\alpha_{lkg}\tilde{\mathbf{s}}_{lkg}\right)\right\} \tag{9}$$

and

$$p(\mathbf{r}_{lk}\,|\,H_0)=C_0\exp\left\{-\frac{1}{2}\mathbf{r}_{l,k}\mathbf{R}_{lk}^{-1}\mathbf{r}_{l,k}\right\} \tag{10}$$

where C_1 and C_0 are constants irrelevant to $\boldsymbol{\theta}$. Up to the fact that $p(\mathbf{r}_{lk}\,|\,H_0)$ is not a function of $\boldsymbol{\theta}$, the likelihood function is rewritten as likelihood ratio:

$$\begin{aligned}p(\mathbf{r}_{lk}|\boldsymbol{\theta},\ \boldsymbol{\alpha}_{lk},H_1)&\propto\frac{p(\mathbf{r}_{lk}|\boldsymbol{\theta},\ \alpha_{lk},H_1)}{p(\mathbf{r}_{lk}\,|\,H_0)}\\&=\exp\left\{\frac{1}{2}\mathbf{r}_{lk}^H\mathbf{R}_{lk}^{-1}\left(\sum_{g=1}^{G}\sqrt{\frac{E}{N}}\alpha_{lkg}\tilde{\mathbf{s}}_{lkg}\right)\right.\\&\quad+\frac{1}{2}\left(\sum_{g=1}^{G}\sqrt{\frac{E}{N}}\alpha_{lkg}\tilde{\mathbf{s}}_{lkg}\right)^H\mathbf{R}_{lk}^{-1}\mathbf{r}_{lk}\\&\quad\left.-\frac{E}{2N}\left(\sum_{g=1}^{G}\alpha_{lkg}\tilde{\mathbf{s}}_{lkg}\right)^H\mathbf{R}_{lk}^{-1}\left(\sum_{g=1}^{G}\alpha_{lkg}\tilde{\mathbf{s}}_{lkg}\right)\right\}\end{aligned} \tag{11}$$

where α_{lkg} is a parameter related to the Radar Cross-Section (RCS) of the gth target, and is unknown before localization in most cases. Thus, the general likelihood ratio is utilized to solve the problem [16]. For any $\boldsymbol{\theta}$, the likelihood (11) is maximized by

$$\frac{\partial}{\partial\boldsymbol{\alpha}_{lk}}\ln p(\mathbf{r}_{l,k}|\boldsymbol{\theta},\ \boldsymbol{\alpha}_{lk},H_1)|_{\boldsymbol{\alpha}_{lk}=\hat{\boldsymbol{\alpha}}_{lkML}}=\mathbf{0} \tag{12}$$

To simplify the problem, we consider a scenario with completely resolved targets first. From *Definition 1* and the fact that $\mathbf{R}_{lk}^{-1}$ is a diagonal matrix, we have

$$\tilde{\mathbf{s}}_{lkg_1}^H\mathbf{R}_{lk}^{-1}\tilde{\mathbf{s}}_{lkg2}=0,\ \ g_1\neq g_2 \tag{13}$$

thus (11) can be rewritten as follows

$$\begin{aligned}p(\mathbf{r}_{l,k}|\boldsymbol{\theta},\ \boldsymbol{\alpha}_{lk},H_1)\propto\exp\{&\frac{1}{2}\mathbf{r}_{lk}^H\mathbf{R}_{lk}^{-1}\left(\sum_{g=1}^{G}\sqrt{\frac{E}{N}}\alpha_{lkg}\tilde{\mathbf{s}}_{lkg}\right)\\&+\frac{1}{2}\left(\sum_{g=1}^{G}\sqrt{\frac{E}{N}}\alpha_{lkg}\tilde{\mathbf{s}}_{lkg}\right)^H\mathbf{R}_{lk}^{-1}\mathbf{r}_{lk}\\&-\frac{E}{2N}\sum_{g=1}^{G}\left|\alpha_{lkg}\right|^2\tilde{\mathbf{s}}_{lkg}{}^H\mathbf{R}_{lk}^{-1}\tilde{\mathbf{s}}_{lkg}\}\end{aligned} \tag{14}$$

Plugging (14) into (12), the ML estimation of α_{lkg} is

$$\hat{\alpha}_{lkgML}=\frac{\tilde{\mathbf{s}}_{lkg}^H\mathbf{R}_{lk}^{-1}\mathbf{r}_{lk}}{\sqrt{\frac{E}{N}}\tilde{\mathbf{s}}_{lkg}\mathbf{R}_{lk}^{-1}\tilde{\mathbf{s}}_{lkg}^H} \tag{15}$$

Substituting the ML estimation of $\boldsymbol{\alpha}_{lk}$ and $\mathbf{R}_{lk}^{-1}=1/\sigma_{lk}^2\mathbf{I}$ into the likelihood function (14), we have

$$\ln p(\mathbf{r}_{lk}|\boldsymbol{\theta},\ \ H_1)\propto\frac{E}{N}\sum_{g=1}^{G}\frac{1}{\sigma_{lk}^2}\left|\tilde{\mathbf{s}}_{lkg}^H\mathbf{r}_{lk}\right|^2 \tag{16}$$

Employing the assumption that $\mathbf{n}_{lk}$ are independent across different paths (indexed by lk), the ML joint estimation of locations all the targets is

$$\hat{\boldsymbol{\theta}}_{ML}=\underset{(\boldsymbol{\theta}_1,\cdots\boldsymbol{\theta}_G)\in S^G}{\arg\max}\sum_{k=1}^{N}\sum_{l=1}^{M}\sum_{g=1}^{G}\frac{1}{\sigma_{lk}^2}\left|\tilde{\mathbf{s}}_{lkg}^H\mathbf{r}_{lk}\right|^2=\underset{(\boldsymbol{\theta}_1,\cdots\boldsymbol{\theta}_G)\in S^G}{\arg\max}\sum_{g=1}^{G}F(\boldsymbol{\theta}_g) \tag{17}$$

Defining $F(\boldsymbol{\theta}_g)$ as follows

$$F(\boldsymbol{\theta}_g)=\sum_{k=1}^{N}\sum_{l=1}^{M}\frac{1}{\sigma_{lk}^2}\left|\tilde{\mathbf{s}}_{lkg}^H\mathbf{r}_{lk}\right|^2 \tag{18}$$

However, the assumption that all the targets are *completely resolved* is usually too stringent for realistic problems. For the more general cases, targets located arbitrarily may share range bins with each other in one or more transmit-receive paths, i.e., unresolved. In this case, the likelihood of the *lk*th path is still formulated as (11), however, because of the existence of some cross-product term $\tilde{\mathbf{s}}_{lkg_1}^H \mathbf{R}_{lk}^{-1} \tilde{\mathbf{s}}_{lkg2} \neq 0,\ g_1 \neq g_2$, it is difficult to get close-form solution of the ML estimation of α_{lkg}. For purpose of obtaining a close-form expression of general likelihood, (15) is still in use as an approximate solution of $\hat{\alpha}_{lkgML}$, and thus the ML estimation of $\boldsymbol{\theta}$ remains the same as (17). In this case, we refer to the high dimensional method formulated in (17) as optimal and can be seen as a theoretical upper bound compared with the following described suboptimal algorithms which may have further performance loss.

The implementation of (17) is involved with a high-dimensional joint maximization. In order to find the global maximum, a 2*G*-dimensional grid search is employed through the whole data plane to find an approximate maximum point, then standard optimization methods can be utilized to refine the estimation [7]. In addition, the approximation of $\hat{\alpha}_{lkgML}$ may lead to considerable performance loss when targets share common range bins in more than a few of the $M \times N$ paths. Besides, this algorithm suffers from the following two problems:

- When the number of targets increases, the high-dimensional grid search process becomes computationally prohibited due to the curse of dimensionality.

- The number of targets has to be predetermined before implementing the multi-target detection and localization, otherwise a multi-hypothesis testing [12] detector is required which further increases the algorithm complexity.

The above problems heavily restrict the applications of the high-dimensional method. Hence, suboptimum algorithms are also investigated in the subsequent sections to trades algorithm performance for implementation complexity.

B. Suboptimum algorithm for partially resolved targets

The aim of this section is to derive reduced-complexity strategies for implement of the MLE (17). The main idea is to split the joint maximization into G disjoint optimization problems by clearing the interference from previously declared targets, which allows information of each target to be extracted one-by-one from the original received signal mingled with information of all the G targets.

Based on the pairwise independence among $\boldsymbol{\theta}_g$, $g = 1, 2, \ldots, G$ (Assume the number of targets is predetermined before localization), we define

$$J = \max_{(\boldsymbol{\theta}_1, \cdots \boldsymbol{\theta}_G) \in S^G} \sum_{g=1}^{G} F(\boldsymbol{\theta}_g) = \sum_{g=1}^{G} \max_{(\boldsymbol{\theta}_1, \cdots \boldsymbol{\theta}_G) \in S^G} F(\boldsymbol{\theta}_g) \tag{19}$$

The suboptimum solution relies on the fact that J can be lower bounded as follows in view of the possibility that some targets are not isolated in each path

$$J \geq \sum_{g=1}^{G} \max_{\boldsymbol{\theta}_g \in S} \left[F(\boldsymbol{\theta}_g) - \sum_{g_d=1}^{g-1} \sum_{k=1}^{N} \sum_{l=1}^{M} F_{lkg_d}(\boldsymbol{\theta}_g) \right] = \sum_{g=1}^{G} \max_{\boldsymbol{\theta}_g \in S} \mathcal{F}_g(\boldsymbol{\theta}_g) \tag{20}$$

where $\mathcal{F}_g(\boldsymbol{\theta}_g)$ is the objective function of the *g*th target and $F_{lkg_d}(\boldsymbol{\theta}_g)$ is defined as modified term related to the previously declared target g_d in the *lk*th path.

$$F_{lkg_d}(\boldsymbol{\theta}_g) = \begin{cases} \dfrac{1}{\sigma_{lk}^2} \left| \tilde{\mathbf{s}}_{lkg}^H \mathbf{r}_{lk} \right|^2 & \boldsymbol{\theta}_g \in \hat{R}_{lkg_d} \\ 0 & \boldsymbol{\theta}_g \notin \hat{R}_{lkg_d} \end{cases} \tag{21}$$

$\hat{R}_{lkg_d}$ is defined as the range containing the interference from the previously declared target g_d. Taking the estimation error of $\hat{\boldsymbol{\theta}}_g$ into consideration, the correctness of the decision of range bins in each path is not guaranteed, thus, $\hat{R}_{lkg_d}$ is defined as follows:

$$\hat{R}_{lkg_d} = \{(x,y) \,|\, [\left\lfloor \left(\sqrt{(x-x_k^t)^2 + (y-y_k^t)^2} \big/ c + \sqrt{(x-x_l^r)^2 + (y-y_l^r)^2} \big/ c \right) \Big/ \tau_c \right\rfloor - \left\lfloor \hat{\tau}_{lkg_d} / \tau_c \right\rfloor] \leq 1\} \tag{22}$$

where $\hat{\tau}_{lkg_d}$ is the time delay of the target located at $\hat{\boldsymbol{\theta}}_{g_d}$ in the *lk*th path, τ_c is the effective duration of the time-correlation function of the transmitted waveform and $\lfloor \bullet \rfloor$ is the maximum integer not greater than $\bullet$.

The inequality in (20) simply follows the fact that the locations $\hat{\boldsymbol{\theta}}_1, \ldots, \hat{\boldsymbol{\theta}}_G$ are contained in the maximization set of (17) and all the modified terms ($F_{lkg_d}(\boldsymbol{\theta}_g)$) are greater than zero. From the definition above, it is obvious that the modified term indicates the information belonging to the paths in which the search point and previously declared targets are not isolated. Thus, the redefined objective function $\mathcal{F}_g(\boldsymbol{\theta}_g)$ only contains the information of the paths in which targets are isolated. Now we have the estimation of $\boldsymbol{\theta}_g$ that

$$\hat{\boldsymbol{\theta}}_g = \arg\max_{\theta_g \in S} \mathcal{F}(\boldsymbol{\theta}_g) \tag{23}$$

The implementation of (23) is involved with an optimization in the original 2-dimensional space, and thus reducing the searching dimension significantly compared with the optimal high dimensional method.

In order to solve the multi-target localization problem from (20), an iterative way of which the spirit is similar to the CLEAN algorithm [13] is introduced. Without loss of generality, the localization process starts with the strongest target (defined as target 1), and the remaining $(G-1)$ targets are localized one by one from the strongest target to the weakest one by repeating the searching process formulated in (23). In this case, the multi-target problem is degenerated to several single target localization problems, since the local peaks caused by echoes from other undetermined targets (say target q, $q > g$) are regarded as background noise in the localization process, and the information of previously declared targets have been eliminated from the objective function $\mathcal{F}_g(\boldsymbol{\theta}_g)$.

Unlike single target localization, a detection process is utilized to decide whether the local peak $\mathcal{F}_g(\hat{\boldsymbol{\theta}}_g)$ is caused by the echo from a target or background noise. When all of the G estimated locations have been determined, a joint decision is made as follows

$$\sum_{g=1}^{G} \mathcal{F}_g(\hat{\boldsymbol{\theta}}_g) \underset{H_1}{\overset{H_0}{\lesseqgtr}} \lambda \tag{24}$$

where λ is a set threshold related to the background noise in the whole search space and the required false alarm probability with H_1 corresponding to the G targets presence hypothesis located at $\{\boldsymbol{\theta}_1, \boldsymbol{\theta}_2, ..., \boldsymbol{\theta}_G\}$ respectively and H_0 corresponding to the noise only hypothesis.

To simplify the detection, we transform (24) into G disjoint single target detection problem. Owing to the fact that the statistical function ($\mathcal{F}_g(\hat{\boldsymbol{\theta}}_g)$) of each target only consists of paths having been removed of the interference of declared targets, single target detection is reasonable based on $\mathcal{F}_g(\hat{\boldsymbol{\theta}}_g)$.

$$\mathcal{F}_g(\hat{\boldsymbol{\theta}}_g) \underset{H_1'}{\overset{H_0'}{\lesseqgtr}} \lambda_g, \ \ g = 1, 2, ..., G \tag{25}$$

where λ_g is the threshold for target g. The threshold is determined by the background noise in neighboring range of $\hat{\boldsymbol{\theta}}_g$ and the required false alarm probability with H_1' corresponding to the target presence hypothesis located at $\hat{\boldsymbol{\theta}}_g$ and H_0' corresponding to the noise only hypothesis. Noting that λ_g is in relation to the number of paths contained in the corresponding statistical function $\mathcal{F}_g(\hat{\boldsymbol{\theta}}_g)$, λ_g is also related to $\hat{\boldsymbol{\theta}}_g$.

However, the number of targets is usually unknown before the localization, thus (24) is no longer realizable, instead, we are faced with a multi-hypothesis testing problem with difficulty to compute. Luckily, the disjoint detection remains valid because we judge every target separately, and the statistical function of each target only consists of paths having been removed of the interference of declared targets. Noticing that the threshold of each detection changes with the target location, the no target determination in the G_1 th estimated location does not guarantee that $\mathcal{F}_{G_1}(\hat{\boldsymbol{\theta}}_{G_1})$ ($G_2 > G_1$) is lower than the corresponding threshold λ_{G_2} although we determine the targets from the strongest one to the weakest one. To solve this problem, we set an upper bound of the number of the potential targets $G_{\max}$ depends on the maximum handling capacity of the processor, thus the iteration ends when $G_{\max}$ estimated locations have been obtained.

To summarize, this proposed suboptimum algorithm works in an iterative way which has an estimation step (containing an elimination process and an optimization process) and a detection step in each iteration. It extracts the information of each target one-by-one from the raw signal wherein the stronger target is dealt with earlier until meeting the aforementioned terminal condition. In this way, we refer to this joint detection and localization algorithm as successive-interference-cancellation (SIC) multi-target localization algorithm and the procedures of the algorithm are shown in TABLE I. In fact, the idea of joint detection and parameter estimation for statistical MIMO radar was mentioned before in [17]. However, it only dealt with a single extended target instead of multi-target. Moreover, considering the difference between the proposed SIC multi-target localization algorithm and the SIC algorithm used in communication problems such as multipath and multi-user, the former subtracts the contribution of the estimated targets from the objective function (or the statistical function) whereas the latter cancels the interference in the received signal.

TABLE I. THE PROCEDURES OF SIC MULTI-TARGET LOCALIZATION ALGORITHM

1) Initialization: $g = 1$, for all $\boldsymbol{\theta}_g \in S$, objective function $\mathcal{F}_g(\boldsymbol{\theta}_g) = F(\boldsymbol{\theta}_g)$.

2) Eestimation step:

- Elimination process: remove the interference of the extracted target.
- Optimization process: for all $\boldsymbol{\theta}_g \in S$, obtain the maximum likelihood estimation

$$\hat{\boldsymbol{\theta}}_g = \arg\max_{\theta_g \in S} \mathcal{F}_g(\boldsymbol{\theta}_g) \tag{26}$$

and the threshold λ_g corresponding to $\hat{\boldsymbol{\theta}}_g$.

3) Detection step: if $\mathcal{F}_g(\hat{\boldsymbol{\theta}}_g) > \lambda_g$,

- Add the estimation of the gth target $\hat{\boldsymbol{\theta}}_g$ in the declared target collection,
- Determine the removing range by (22) based on the declared target collection.

Go to step *2)* and $g = g + 1$.

4) If $g \le G_{\max}$, repeat step *2)* and step *3)*.

C. *Suboptimal algorithm for completely resolved targets*

When targets are completely resolved, the proposed SIC multi-target localization algorithm can be simplified further. For this scenario, a different lower bound of J can be obtained below

$$J \ge \sum_{g=1}^{G} \max_{\boldsymbol{\theta}_g \in S \backslash u_g} F(\boldsymbol{\theta}_g) \tag{27}$$

where $u_g = \{\hat{R}_1, \hat{R}_2, ..., \hat{R}_{g-1}\}$. And $\hat{R}_g$ contains the regions defined in (22) for all the $M \times N$ paths. The estimation of the location of a certain target is determined by

$$\hat{\boldsymbol{\theta}}_g = \arg\max_{\theta_g \in S \setminus u_g} F(\boldsymbol{\theta}_g) \tag{28}$$

Assuming that different targets fall in different range bins in any path, a conclusion is formulated that the location of the pth ($p \neq g$) target will not be included in the area of $\hat{R}_g$ most likely. Hence, eliminating $\hat{R}_g$ from the searching range will not change the result of $\hat{\boldsymbol{\theta}}_p$.

Now considering a disjoint detection, the existence of a certain target in any estimated location is irrelevant to other targets for the assumption that the targets are isolated in any path. Thus make G joint single target detection process as follows:

$$F(\hat{\boldsymbol{\theta}}_g) \underset{H_1'}{\overset{H_0'}{\lesseqgtr}} \lambda_g, \quad g = 1,2,...,G \tag{29}$$

where λ_g is threshold of the gth target. In most cases, these targets are located within a relatively small range with a background noise differs little in the whole surveillance region, meaning that these thresholds λ_g , $g = 1,2,...,G$ can be simplified into one threshold λ' .

As for conditions that the number of targets is not available before localization, the localization process can be terminated if the G_1 th estimated location is determined as no target. It simply relies on the fact that $F(\boldsymbol{\theta}_{G_1+1}) \leq F(\hat{\boldsymbol{\theta}}_{G_1})$ is efficient, and thus $F(\boldsymbol{\theta}_{G_1+1}) \leq F(\hat{\boldsymbol{\theta}}_{G_1}) < \lambda'$, meaning that every point in the remained search space is decided as H_0 . We refer to this joint detection and localization algorithm as successive-search-space-removing (SSR) multi-target localization algorithm.

D. Comparison of the proposed two suboptimal algorithms

From the aforementioned derivation of the two proposed algorithms, when deals with completely resolved targets, it is obvious that the SIC algorithm is equivalently efficient. On the other hand, the performance of the SSR algorithm in scenario with partially resolved targets is not guaranteed, because the corresponding likelihood local peak may be located outside the search space in the iteration. Thus the localization precision and detection probability of this target are exacerbated severely compared to the SIC algorithm. However, the SSR algorithm reduces search space during each iteration and does not need to compute the modified term. Hence it has less calculation compared with the SIC algorithm. In addition, owing to the different termination strategy, the number of loops drops noteworthily when $G_{\max} \gg G$ (G is the actual number of targets), which also decreases calculation and reduces the false alarm of SSR algorithm to some extent compared with SIC algorithm.

We have already proposed a multi-target localization algorithm in [11], which localizes targets in parallel with the utilization of connected region. Just as aforementioned, a theoratical value of the threshold is not avaliable. If the threshold is set based on theory of target detection, the searching range of different targets may be connected with others (as shown in Fig.2(a)) and thus it is no longer able to separate targets successfully. This phenomenon apears when the signal-to-noise ratio (SNR) is high, since the detection threshold under this condition is much less than the maximum in the whole data plane. On the other hand, in consideration of the resolution of MIMO radar [14], the threshold is set to be -3dB (half) of the global maximum, and the searching ranges are shown in Fig. 2(b) when the proportion of the target intensity is 1:0.65:0.5 and the SNR is 10dB. In Fig. 2(b), the weakest target located at (15, 16) km is missing, which demonstrates that weak targets may be covered up by strong targets in this case. However, according to the proposed numerical examples in Section IV, SIC and SSR algorithm delcared all the targets successfully in high SNR conditions and weak targets are not covered up by strong targets.

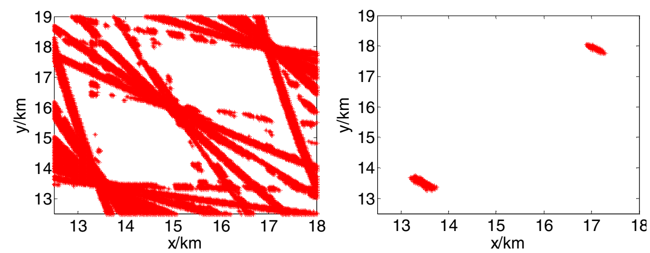

(a) (b)

Fig. 2. Ranges in which pixel value pass the threshold which is set (a) based on theory of target detection (b) to be -3dB of the global maximum when SNR=10dB

As for the 'ghost target' problem mentioned in [15], which is a kind of false target resulted from the combination of measured ranges that do not belong together. In fact, Our previous algorithm is still faced with this problem as shown in Fig. 3 with at least three 'ghost targets' (marked by red or blue ellipse). Compared with the simulation results of the proposed two algorithms in Section IV, the algorithms declare anveragely less than one false targets against SNR from -15dB to 15dB, indicating significant reduction of 'ghost targets'.

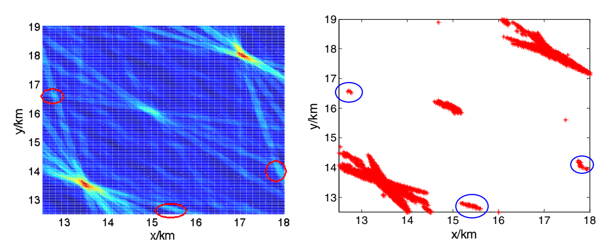

(a) (b)

Fig. 3. (a) Likelihood in the whole data plane (b) Ranges in which pixel value pass the threshold when SNR=5dB

IV. SIMULATION RESULTS

A. Simulation of SIC algorithm for partially resolved targets

In this section, a scenario with three targets and a 5×5 MIMO radar system is designed to assess the performance of the proposed SIC algorithm. Each antenna is a transmitter and receiver at the same time. The placement of the radar antennas and targets are shown in Fig. 4. The three targets are located at (13.5, 13.5) km, (17, 18) km, (13.36, 16.48) km, respectively. The targets positions are carefully chosen such that the 1st target and 3rd target are unresolved in some paths. The proportion of the target intensity is 1:0.65:0.5 to find whether the weak target will be covered up by strong target in the detection process of SIC algorithm. The signal mingled with the echoes of all the three targets are used to define SNR in the simulation. Besides, the performance measurements used are the number of valid target detections and the root mean square (RMS) errors of estimated target positions. To be specific, we define the declared target with an estimated location within 200m of the actual target location both in the two dimensions respectively as a valid target. In the following analysis, the results are gathered by averaging over 1000 realizations.

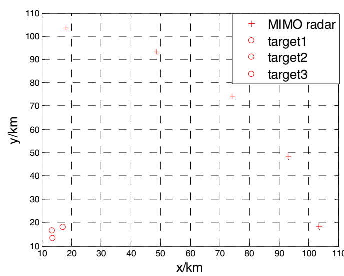

Fig. 4. The placement of MIMO radar system

The performance of the proposed SIC algorithm is shown in Fig. 5~Fig. 6. The detection threshold is adaptive to the number of paths contained in the statistical function of each target. The upper bound of the number of the potential targets is set as $G_{\max} = 5$. In Fig. 5, the performance comparison of SIC and SSR algorithms are given. From Fig. 5(a), it can be seen that the SIC algorithm performs well when SNR is high, specifically, it can correctly declared all the three targets when SNR is greater than 5dB. The numbers of false targets are all below 0.26 when SNR changes from -15dB to 15dB. In Fig. 5(b), the detection probability P_d of all targets is plotted against SNR from -15dB to 15dB for $P_{fa} = 10^{-1}$. As expected, for SIC algorithm, the detection probability of all targets rises towards 1 as the SNR goes up and at the same time, the stronger target corresponds to higher detection probability than weaker target. As for SSR algorithm, it is clear that the 3rd target (which is the weakest and share common range bins with 1st target in some paths) has a great performance loss especially in high SNR conditions. In Fig. 6, based on SIC algorithm, the RMS position errors of all three targets are plotted against SNR from -10dB to 15dB for both x and y dimensions. Note that the level of RMSE unnecessarily follows the intensity order of the targets especially when target SNR is high. The reason is that in high SNR condition, the RMS errors are very close to the Cram´er-Rao Bounds (CRB) affected by ambiguity function which strictly depends on the geometry [8]. Moreover, the RMS error change little when SNR rises from 10dB to 15dB because only grid search is utilized in the simulation, meaning that the grid width may restrict the localization accuracy especially when SNR is high.

The simulation results show that compared with SSR algorithm the SIC algorithm can accurately estimate the number of targets and localizes them with quite high precision even some targets are not isolated in some paths.

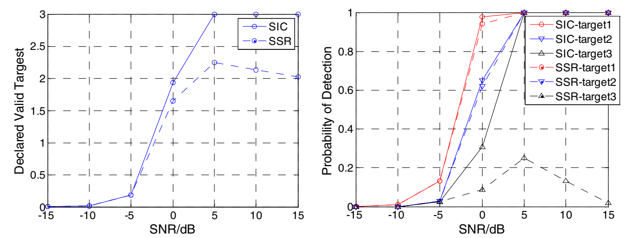

(a) (b)

Fig. 5. (a) The number of valid targets (b) The detection probability P_d of all targets are plotted against SNR from -15dB to 15dB

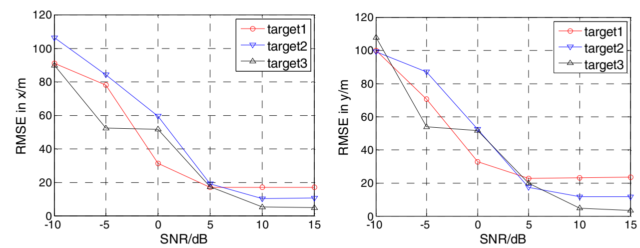

(a) (b)

Fig. 6. The RMS position errors in (a) x dimension and (b) y dimension of all targets are plotted against SNR from -10dB to 15dB for $P_{fa} = 10^{-2}$

B. Simulation of SSR algorithm for completely resolved targets

In this section, the radar placement remains the same while the target locations are changed to (13.5, 13.5) km, (17, 18) km, (15, 16) km to make sure that all targets are completely resolved. The proportion of the target intensity is still 1:0.65:0.5.

The performance of the proposed SSR algorithm is shown in Fig. 7 and Fig. 8 for $P_{fa} = 10^{-2}$. They all show the generally same tendency of SIC algorithm as Fig. 5 and Fig. 6. Compared with the simulation results of the two proposed algorithms in scenario with partially resolved or completely resolved targets respectively, SIC performs well even targets are not isolated in some paths while SSR is efficient only for completely resolved targets.

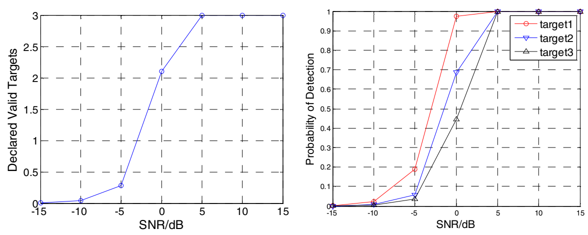

(a) (b)

Fig. 7. (a) The number of valid targets (b) The detection probability P_d of all targets are plotted against SNR from -15dB to 15dB

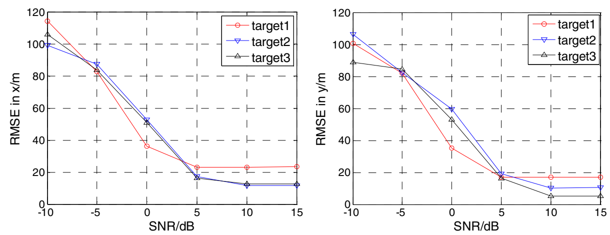

(a) (b)

Fig. 8. The RMS position errors in (a) x dimension and (b) y dimension of all targets are plotted against SNR from -10dB to 15dB for $P_{fa} = 10^{-2}$

V. Conclusion

In this paper, we consider the detection and locating of multiple targets in a noncoherent statistical MIMO system. To combat the troublesome high-dimensional optimization problem of simultaneously estimating multiple targets' positions, we propose two algorithms to sub-optimally split the joint maximization into several disjoint optimization problems, i.e., one corresponding to each prospective target. In this way, the proposed algorithms have much lower complexity compared with the original high-dimensional estimation method. Besides, during the detection and locating process, the proposed algorithms sequentially perform single target detection at each estimated position after eliminating the interference in all the paths from previously declared targets, and the recursive process stops automatically if no target estimate of current stage can exceed the detection threshold. Therefore the multi-hypothesis testing detector is no longer needed when the number of targets is unknown. Simulation results show that the proposed algorithms can correctly estimate the number of targets and localize them with a quite high accuracy when the SNR is high. In particular, the proposed SIC algorithm works well even when some targets are not isolated in some paths.

Acknowledgment

This work was supported by National Natural Science Foundation of China (61201276, 61178068 and 61301266), Fundamental Research Funds of Central Universities (ZYGX2012Z001, ZYGX2012YB004 and ZYGX2013J012), Program for New Century Excellent Talents in University (A1098524023901001063) and China Postdoctoral Science Foundation (2014M550465).

References

[1] B. Lya and J. Abrikian. "Target detection and localization using MIMO radars and sonars."*IEEE Trans. Signal Process.*, vol. 54, no. 10, pp. 3873-3883, 2006.

[2] E. Fishler, A. Haimovich, R. Blum, D. Chizhik, L. Cimini, and R. Valenzuela, "MIMO radar: an idea whose time has come," in *IEEE Radar Conf.*, pp. 71-78, April 2004.

[3] N. H. Lehmann, E. Fishler, A. M. Haimovich, et al. "Evaluation of transmit diversity in MIMO-radar direction finding."*IEEE Trans. Signal Process.*, vol. 55, no. 5, pp. 2215-2225, 2007.

[4] A. M. Haimovich, R. S. Blum, and L. J. Cimini. "MIMO radar with widely separated antennas."*IEEE Signal Process. Mag.,* vol. 25, no. 1, pp 116-129, 2008.

[5] J. Mason, "Algebraic two-satellite TOA/FOA position solution on an ellipsoidal Earth", *IEEE Trans. Aerosp. Electron. Syst.,* vol. 40, no. 3, pp. 1087-1092, 2004.

[6] Q. He, R. S. Blum, and A. M. Haimovich. "Noncoherent MIMO radar for location and velocity estimation: More antennas means better performance." *IEEE Trans. Signal Process.,* vol. 58, no. 7, pp 3661-3680, 2010.

[7] R. Niu, R. S. Blum, P. Varshney and A. Drozd. "Target localization and tracking in noncoherent multiple-input multiple-output radar systems." *IEEE Trans. Aerosp. Electron. Syst.,* vol. 48, no.2, pp. 1466-1489, 2012.

[8] H. Godrich, A. M. Haimovich and R. S. Blum. " Target localization accuracy gain in MIMO radar-based systems" *IEEE Trans. Inform. Theory*, vol. 56, no, 6, pp. 2783-2803, 2010.

[9] M. Greco, F. Gini, P. Stinco, A. Farina "Cramér-Rao bounds and selection of bistatic channels for multistatic radar systems", *IEEE Trans. Aerosp. Electron. Syst.,* vol. 47, no.4, pp. 2934-2948, 2011.

[10] A. A. Gorji, R. Tharmarasa, T. Kirubarajan "Widely Separated MIMO versus Multistatic Radars for Target Localization and Tracking" , *IEEE Trans. Aerosp. Electron. Syst.,* vol. 49, no. 4, pp. 2179 – 2194, 2013

[11] Y. Ai, W. Yi, G. Cui and L. Kong. "Multi-target localization for noncoherent MIMO radar with widely separated antennas" in *IEEE radar conf .(RADAR)*, 2014, accepted.

[12] T. Schonhoff, A. A. Giordano."Detection and Estimation Theory and its applications". PearsonPrentice Hall, 2006.

[13] B. G. Clark, "An efficient implement of the algorithm 'CLEAN' ", *Astron. Astrophs.*, vol. 89, pp. 377-378, 1980

[14] Doughty, Shaun Raymond. "Development and performance evaluation of a multistatic radar system", Diss. University of London, 2008.

[15] Folster, Florian, and Hermann Rohling. "Data association and tracking for automotive radar networks."*IEEE Trans. Intell. Transp. Syst.,* vol. 6, no. 4,pp. 370–377, 2005.

[16] Q. He, R. S. Blum, H. Godrich and A. M. Haimovich, "Target velocity estimation and antenna placement for MIMO radar with widely separated antennas", *IEEE J. Sel. Top. Signal Process.*, vol. 4, no.1, pp. 79-100, 2010.

[17] A. Tajer, G. H. Jajamovich, X. Wang and G. V. Moustakides, "Optimal joint target detection and parameter estimation by MIMO radar". *IEEE J. Sel. Top. Signal Process.*, vol. 4, no.14, pp. 127-145, 2010